Acta Geochim (2021) 40(4):623–639
https://doi.org/10.1007/s11631-021-00462-6

ORIGINAL ARTICLE

Geochemical constraints and uranium potential of the younger granitic rocks in El Maghrbia area, Central Eastern Desert, Egypt

A. E. El-Kammar[1] · A. H. El-Afandy[2] · T. Nasr[2] · M. Coltorti[3] · F. Casetta[3]

Received: 11 November 2020 / Revised: 7 January 2021 / Accepted: 4 February 2021 / Published online: 22 March 2021

Abstract The present work deals with the mineralogy, geochemical behavior and uranium potentiality of the monzogranites of El Maghrbia area, which comprise G. El Maghrbia and G. El Eredyia and situated in the central Eastern Desert of Egypt. G. El-Erediya monzogranites represents a promising area for uranium mineralizations. These granites have shear zone filled with red and black silica veins containing many radioactive anomalies with visible yellow secondary uranium minerals. The shear zone is highly affected by different degrees of alterations such as silicification, kaolinitization, sassuritization and ferrugination. Monzogranites of El-Erediya area possess higher values of their radioactivity than in El Maghrbia monzogranites in which eU and eTh, reaches up to 792.3 and 66.81 ppm, whilst average content of eU and eTh in El Maghrabia granites are 3.86 and 8.55 ppm, respectively owing to the presence of radioactive minerals such as uraninite, uranothorite, uranophane, kasolite, betafite, zircon and monazite. Intensive geochemical analyses indicated that, the studied monzogranites are distinctly anomalous in U, where the average U is more than 620-fold the Upper Continental Crust (UCC), marked enrichment (> tenfold) of the elements Cd, Mo, Pb, Bi, Nb and W. The Th/U ratio decreases from 2.8, as a chondritic value, to 0.0023 for the studied granites, proposing extreme fractionation towards an extensive secondary migration-in of U. The Zr and Hf are depleted in the studied granites relative to the UCC, whereas Nb and Ta are strongly enriched. The content of Y is about sixfold enriched which reflects relative enhancement of the HREE during the alteration processes. Uranium correlates with $Fe_2O_3^T$, suggesting a possible association between uranium and ferrugination. Thus, the occurrences of uranium are epigenetic by remobilization from the host rock to the sheared zones, probably through metasomatic process where U–Fe–Mg replaced the feldspars in an oxidized condition. The high levels of radioactivity in the rocks being studied it them a priority for discovery and expanding the potentiality of the highly mineralized localities.

Keywords Potentiality · Uranium · Geochemistry · El Maghrabia · El Erediya · Egypt

✉ T. Nasr
taher15988@gmail.com

A. E. El-Kammar
amkammar@hotmail.com

A. H. El-Afandy
adel_elafandy@hotmail.com

M. Coltorti
massimo.coltorti@unife.it

F. Casetta
cstfrc@unife.it

[1] Department of Geology, Faculty of Science, Cairo University, Cairo, Egypt

[2] Nuclear Materials Authority, El Maadi, Cairo, Egypt

[3] Department of Physics and Earth Sciences, University of Ferrara, Ferrara, Italy

1 Introduction

It's known that granites are one of the most favorable host rocks for U-mineralization in the world, especially those of peraluminous two-mica granites (Cuney et al. 1984; Poty et al. 1986; Friedrich et al. 1989). The YG constitute about third of the plutonic assemblage in the Egyptian Shield (Fig. 1a). Some of these granites are associated with a major part of the radioactive anomalies due to host most

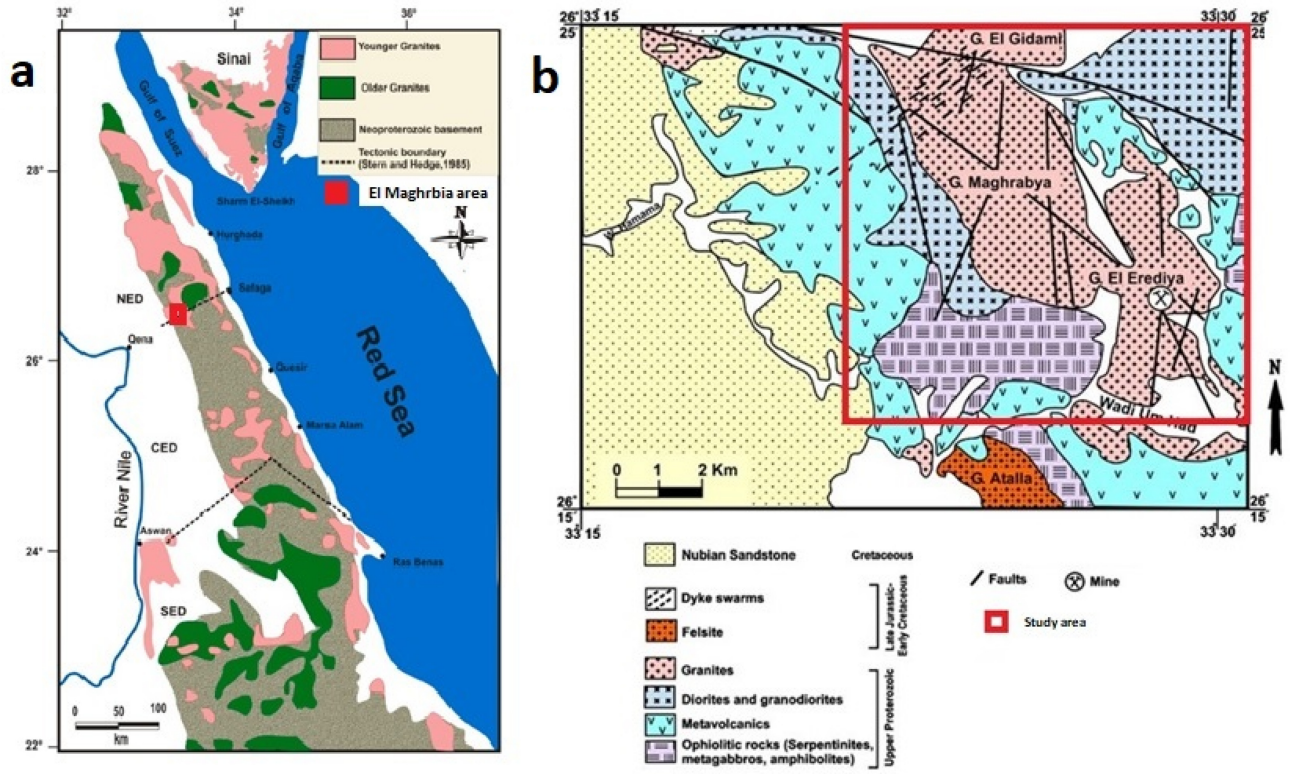

Fig. 1 **a** Distribution map of the Egyptian Older and Younger Granites within the Neoproterozoic basement of the Eastern Desert and Sinai (modified after Farahat et al. 2011). **b** Geological map of El Maghrbia area (modified after Abu Dief 1992)

interesting uranium mineralization. The Egyptian younger granites (YG) obtained U–Pb zircon ages (610–580 Ma). Published U–Pb zircon ages (Moussa et al. 2008; Be'eri-Shlevin et al. 2009; Ali et al. 2009a, b, 2012; Eyal et al. 2010; Andresen et al. 2014; Eliwa et al. 2014; Ali 2015; Mahdy et al. 2015; El-Bialy et al. 2020) demonstrated that There are two distinct Ediacaran granitoid suites. Older Granites (OG) and Younger Granites (YG) (Fig. 1a). The YG were emplaced at 601–589 Ma in the post-collisional regime, while the emplacement of the OG had eventuated earlier (ca.10 Ma) at 622–611 Ma.

Some U-mineralizations were recorded related to the younger granites 590–550 Ma (Stern and Hedge 1985). Examples of these mineralizations are restricted to fracture zones within the plutons such as El-Erediya (El Kassas 1974), El Missikat (Bakhit 1978) and Gattar (Salman et al. 1990), in the Central Eastern Desert. Also there is an important disseminated-type U-mineralization was discovered in Um Ara-Um Shilman younger granite pluton at the South Eastern Desert (Abdel Meguid 1986).

Uranium existing in granites can be genetically divided into two types; primary uranium and secondary uranium (Jiashu and Zehong 1982). The former is fixed in rocks during the crystallization of magma; while the latter is precipitated by various geological events later from dissolved and transported uranium, which in turn comes from the primary uranium. The secondary uranium can be subdivided into three types; (1) absorbed uranium in altered minerals such as montmorillonite, chlorite and limonite; (2) interstitial uranium at the grain boundaries which formed as a result of hydrothermal solution migration along the interstices of minerals and (3) uranium in microfractures, the formation of this kind of uranium takes place during the circulation of hydrothermal solution after the deformation of rocks. These three types of secondary uranium are regarded as the final preserved products through all the geological processes such as metasomatism, hydrothermal alteration and weathering.

The geology, structure, mineralogy and geochemistry of the present area were studied by Dardier et al. (2001), Abdallah (2004), Dardier (2004), Abd El-Naby (2007), Raslan (2009). Even though, the mineralization and the geochemical annoniation of radioactive minerals in the monzogranites were not achieved. Accordingly, the present work will shed the light on the petrology, mineralization and geochemical attributes of radioactive minerals associated with the monzogranites at El Maghrbia area in the Central Eastern Desert of Egypt.

2 Geologic setting

The investigated area is located in the Central Eastern. Desert of Egypt between latitudes 26° 18′ 35″ and 26° 24′ 43″ N and longitudes 33° 22′ 11″ and 33° 30′ 42″ E, at 35 km to the south of the midway point on Qena-Safaga road (Fig. 1b). According to the field investigations and petrographic description, the younger granites in the studied area comprise El Maghrbia and El Eredyia monzogranites.

El Maghrbia monzogranites cover the centeral part of the mapped area (Fig. 1b). They are medium to coarse grained having pink, reddish pink to pinkish greyish colors. It shows cavernous, exfoliated, jointed, fractured appearance and spheroidal weathering. The western part of this granite is cutted by mineralized shear zones filled with fluorite veins. Also they contain manganese oxides filling joints and fractures.

El Eredyia monzogranites are located at the Southeastern part of the mapped area (Fig. 1b). It is pink to reddish pink in color, slightly leucocratic and exhibiting low to moderate relief with medium to coarse-grained texture. It shows highly weathered, exfoliated and jointed surfaces caused by weathering processes. These granites have shear zones especially at the southern periphery. The shear zones are filled with red (red jasper) colors and siliceous black veins (smoky quartz). There is a special interest with jasper veins after discovering of several radioactive anomalies with visible yellow. secondary uranium mineralization along the southern fringe of El Eredyia granites (Fig. 2a, b). The walls are stained along the shear zones with reddish brown colors due to ferrugination, light greyish green to whitish buff color due to sericitization and kaolinization and yellowish to dark green coloration due to chloritization and epidotization (Fig. 2b, c). Also, it contains manganese oxides filling joints and fractures (Fig. 2d).

The studied area is dissected by quartz-feldspar porphyry and doleritic dikes. The quartz-feldspar porphyry dikes extend as dike swarms striking in the NE-SW to ENE-WSW directions with nearly vertical dips (Fig. 1b). They cross cut through the north western periphery of G. El Maghrabia and not dissecting the El Eredyia granites. They vary in length from few meters up to eight kilometers and their width is ranging between few centimeters up to 20 m. The doleritic dikes in the study area are trending in NE-SW, NW–SE and E-W directions with vertical and steep inclination; these trends are the same of the fault trends. They are usually straight with gentle curvatures, ranging in thickness between 0.5 and 10 meters, while their lengths extend for few kilometers. They are the youngest dikes in the studied area, especially those trending NW–SE; they invade all rock types even the El Eredyia granites.

The latest event in the area is represented by the intrusion of quartz and jasperoid veins that dissected all rock types within the study area with different magnitudes. The shear zones especially in the southern part of G, El Eredyia are filled with siliceous veins and veinlets of white black (smoky quartz), (milky quartz) and red (red jasper) colors. The black and red silica have abnormal radioactivity (anomalies) with visible uranium mineralizations.

3 Sampling and analytical techniques

For microscopic investigations, fifty thin sections (25 samples from each of El Maghrbia and El Eredyia monzogranites) were prepared to denote their main rock forming minerals and their textures. Heavy minerals, especially rare metal-bearing phases were achieved from low-density minerals through a standard heavy liquid method, using bromoform, then washed and dried. The obtained magnetic and nonmagnetic heavy mineral fractions were investigated under a binocular microscope. SEM image and semi-quantitative analyses of the picked mineral grains were indicated by a Phillips XL 30 Scanning Electron microscope at the laboratory of the Nuclear Materials Authority of Egypt. Thirty samples representing El Eredyia and El Maghrbia monzogranites were chosen from the highly radioactive zones were used for geochemical studies. Major oxides and trace elements were analyzed using XRF (X-ray fluorescent spectroscopy), while rare earth elements were analyzed using. ICP-MS (inductively coupled plasma-mass spectrometry) at the ACME Analytical Laboratory,Vancouver, Canada. Field ground gamma-ray spectrometry survey has been done by using well calibrated and high-sensitive model RS-230 spectrometer. This instrument used to detect dose rate (D.R.) in unit (nano sieverts per hour ($nSvh^{-1}$)), potassium (K%), equivalent uranium content (eUppm), and equivalent thorium content (eTh ppm) on rock outcrops.

4 Results

4.1 Distribution of radioelements in El Maghrbia fresh granites and El Eredyia fresh and altered (anomalous) granites

The minimum, maximum and average distribution of the surface radioelements (eU ppm, eTh ppm), K %, and dose rate (D.R.) as well as some statistics (Standared diviation), in El Maghrbia fresh granites and El Eredyia fresh and altered (anomalous) granites are summarized in (Table 1).

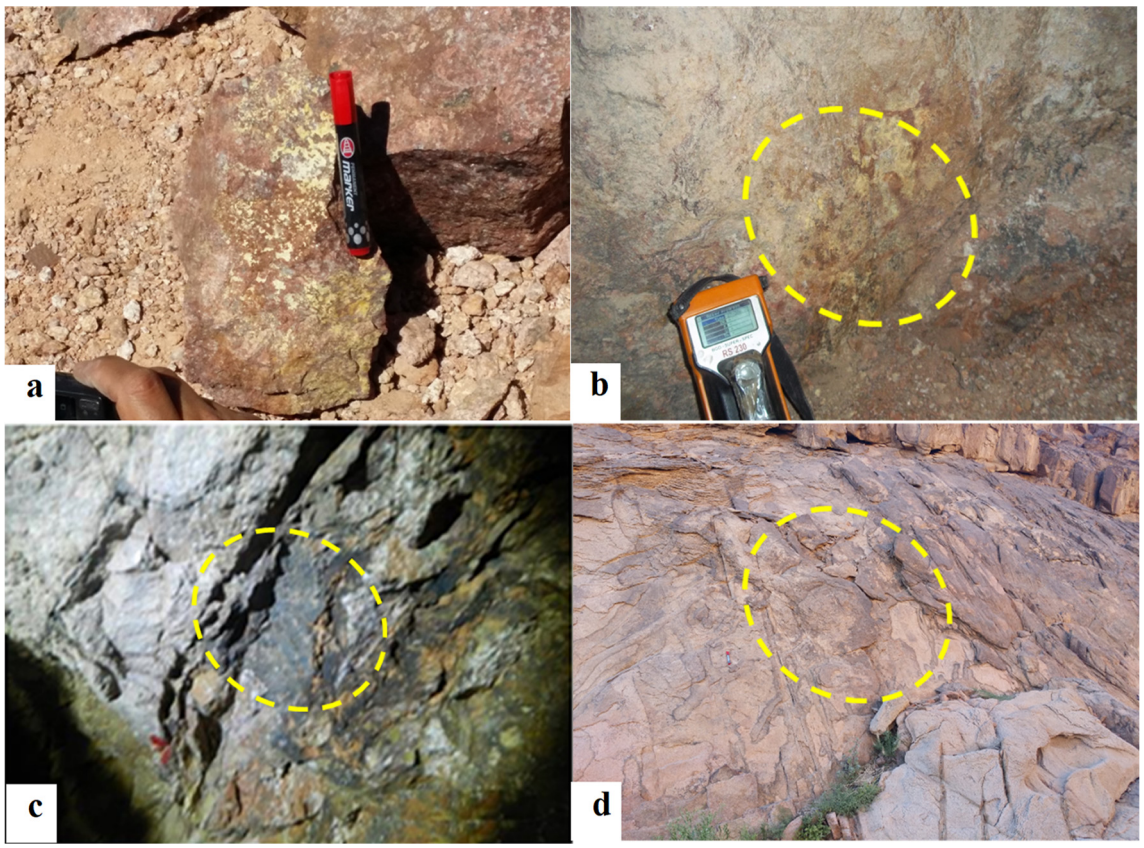

Fig. 2 Photographs of studied area showing: **a** Visible uranium mineral at Eredyia granites. **b** Visible uranium mineralization absorbed with kaolinitization at El Eredyia granites. **c** Ferrugination and kaolinitization at El Eredyia granites. **d** Manganese oxides filling joints and fractures at Eredyia granites (photo looking north)

4.2 Petrography

According to plotting on classification diagram of Streckeisen (1976) based on the relative minerals' abundance is verified that the younger granites are Monzogranites which are represented by El Maghrbia and El Eredyiaplutons. El Eredyia granitic mass is typically bleached, fractured and altered to varying degrees of alterations especially along the major fracture zones and contacts with jasperoid veins. Silicification, kaolinitization,sassuritization and ferrugination are the most common alteration features along major and minor fractures in addition to partial and complete zircon metamictization has been recorded (Fig. 3a, b, c, e, f). Silicification is the earliest and most important alteration feature occur in the studied area. It started with white silica veins and fracture fillings, (Fig. 3e). The second phase of alteration is indicated by rejuvenation of these fractures as indicated by normal faults and by brecciation of the early silica veins as well as the intrusive contacts of this granite. A new uranium-rich red silica solution subsequently cemented the breccia and degraded the early formed pyrites to iron oxides (Fig. 3d, f). The granitic contacts were intensively altered by kaolinitization, sericitization, and ferrugination along parts of early silica veins and fractures.

In some zones, the altered granite was intensively silicified and highly radioactive (Fig. 3d, e, f). Alteration of pitchblende and iron oxides indicates a third alteration event and redistribution process which leached uranium from some of the altered zones, especially the friable unsilicified ones, while the original mineralization is preserved in silicified zones. Most of the high uranium concentrations are associated with the second alteration phase in the cementing red silica of the brecciated contacts, and with the third phase in the alteration zones at the jasperoid veins intersections with the secondary fractures. The U-mineralizations in these zones are essentially primary pitchblende associated with pyrite and/or secondary uranophane with some hematitized iron oxides.

Radioactive minerals are represented by uranothorite which characterized by its brick red color occurring as amorphous and strips crystals included in quartz. Radioactive material has been encountered as filling fractures associated with opaque minerals (Fig. 3d–f).

Table 1 Summary of the statistics for the surface distribution of the K%, eU (ppm), eTh (ppm) and their ratios for studied different rocks

	eU (ppm)	eTh (ppm)	K %	D.R. (μmv/y)	eU/eTh	eTh/K	eU-(eTh/3.5)
EL Eredyia Fresh granite							
Number of values	123.00	123.00	123.00	123.00	123.00	123.00	123.00
Minimum	3.60	6.80	2.90	3.80	0.28	1.41	− 0.14
Maximum	674.00	271.00	6.30	1899.00	19.82	64.88	664.29
Mean	46.32	38.52	4.54	292.35	1.17	8.73	35.32
Standard deviation	116.77	48.69	0.75	219.59	2.97	11.50	113.27
X + 3S	396.64	184.60	6.79	951.11	10.10	43.24	375.14
X − 3S	− 304.00	− 107.56	2.30	− 366.40	− 7.75	− 25.78	− 304.51
El Eredyia altered granite							
Number of values	144.00	144.00	144.00	144.00	144.00	144.00	144.00
Minimum	109.00	8.90	4.10	1.20	3.06	0.88	102.66
Maximum	1345.00	102.00	17.10	987.00	103.26	12.06	1323.29
Mean	792.23	66.81	10.99	103.90	11.47	6.34	773.14
Standard deviation	425.71	22.63	4.14	289.27	8.77	1.55	420.07
X + 3S	2069.37	134.69	23.41	971.71	37.77	10.98	2033.34
X − 3S	− 484.92	− 1.06	− 1.43	− 763.91	− 14.83	1.70	− 487.07
El Maghrbia granite							
Number of values	168.00	168.00	168.00	168.00	168.00	168.00	168.00
Minimum	2.50	5.20	4.10	101.00	0.32	0.95	0.29
Maximum	5.90	10.60	5.60	182.00	0.72	2.52	3.19
Mean	3.86	8.55	4.96	135.09	0.47	1.73	1.42
Standard deviation	0.74	1.60	0.46	18.44	0.11	0.34	0.71
X + 3S	6.09	13.34	6.35	190.40	0.79	2.74	3.54
X − 3S	1.64	3.76	3.57	79.78	0.14	0.72	− 0.70

4.3 Mineralogy and high-resolution grain analysis of the altered monzogranites

A combination of binocular microscope, scanning electron microscope (SEM/EDX) and back-scattered electron imaging (BSE) analysis of heavy minerals associated with the investigated monzogranites clarified the presence of the following radioactive minerals.

4.3.1 Uranophane

It occurs as disseminated spots or massive aggregates of granular forms as well as dense microcrystalline masses. It is characterized by its yellow and lemon-yellow shades with fibrous and radiating acicular habit (Fig. 4a). In general, it is the alteration product of uraninite. EDX analysis data of uranophane are shown in (Table 2).

4.3.2 Uraninite

It occurs as subheral to anhedral grains and exhibit black to grayish black colors with vitreous luster (Fig. 4b). In some polished grains studied under the SEM, two compositionally different phases were recognized in the same crystals with sharp contact between them. The first phase is interpreted as uraninite, while the other represents the alteration phase. EDX analysis data of uraninite are shown in (Table 2).

4.3.3 Betafite

It occurs as brown hexoctahedral crystal found chiefly in the zone of oxidation and weathering derived from the alteration of uraninite or other U- bearing veins. It is characterized by yellow-green tetragonal plates (Fig. 4c) and strong fluorescence in ultraviolet light. EDX analysis data of betafite are shown in (Table 2).

4.3.4 Kasolite

It occurs as translucent to opaque reddish yellow to brownish yellow grains with vitrous luster and characterized by conchiodalfructures (Fig. 4d). Maurice (1982) suggested that kasolite is dimorphous with uranophane and beta-uranophane due to the complete replacement of Ca by

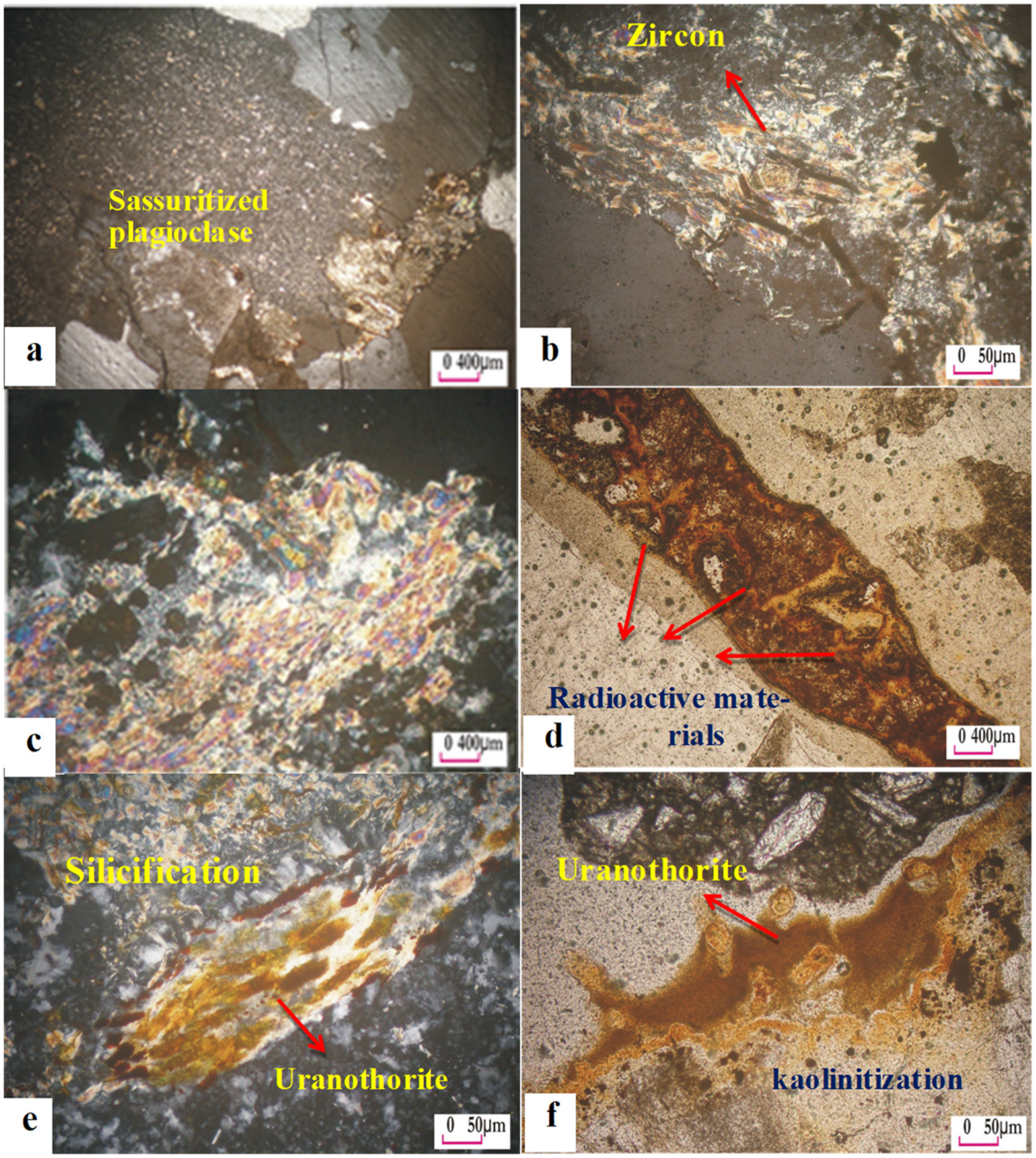

Fig. 3 Photomicrographs of El Eredyia granites: **a** Compleltely sassuritized plagioclase (C.N.). **b** Completely metamectized zircon crystal (C.N.). **c** Sericitization of plagioclase (C.N.). **d** Radioactive material filling fractures. **e** Amorphous crystal of uranothorite associated silicification (C.N.). **f** Amorphous crystal of uranothorite associated kaolinitization

Pb during the high degree of oxidation condition.EDX analysis data of kasolite are shown in (Table 2).

4.3.5 Zircon

It occurs as subhedral to euhedral form. The recorded zircon has yellow, yellowish red to reddish brown colors and sometimes has colorless to pale yellow colors. The majority of zircon grains are transparent and rarely translucent. They are mostly long prismatic grains, while some crystals are short, and have good adamantine luster (Fig. 4e). The EDX analysis data reflect the preponderance of zircon (Table 2). It shows that it is composed essentially of Zr and Si. Other elements are present in small to minor amounts. The Hf, Th and U substitute in small amounts for part of Zr. Some grains show absence of U, Th and Hf.

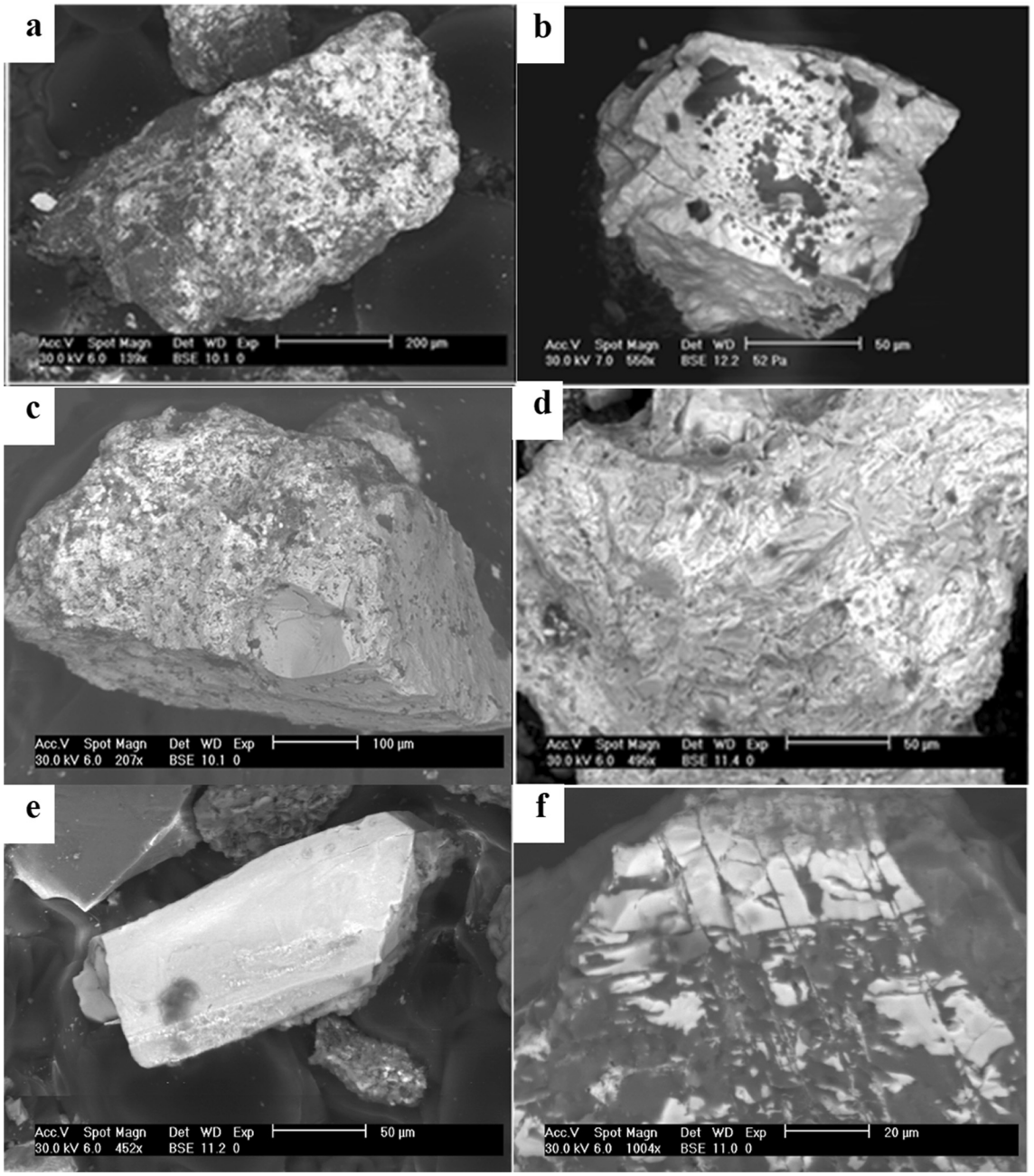

Fig. 4 Photomicrographs and BSE images of uranium mineralization of El Eredyia granite: **a** Uranophane. **b** Uraninite

4.3.6 Monazite

It occurs as lemon yellow, honey yellow to colorless very fine grains. The grains are well rounded mostly oval in shape (Fig. 4f). It is essentially anhydrous orthophosphate of the cerium and the lanthanum group of the rare earth element. The REE are detected as fracture filling or coating of the monazite grains. EDX analysis data reflect the preponderance of monazite (Table 2).

5 Geochemical annotations

This study is based on data of complete chemical analyses of major and trace elements of 30 fresh and metasomatized highly differentiated granites from El Maghrabi and EL Eredyia granitic plutons, northern Eastern Desert of Egypt, (Table 3). The statistics and data reduction provide important clues on the alteration processes. The following is a brief discussion on the obtained output of the statistical treatment done by the SPSS© program.

Table 2 EDX analysis data of secondary uranium minerals (oxygen and carbon are excluded from the analysis for their low precision)

	Elements wt%	Zircon		Elements wt%	Monazite	Elements wt%	Uranophane
	Al	2.93		Al	0.0	Al	1.82
	Si	18.95		Si	2.52	Si	16.06
	Th	0.81		P	22.69	K	1.98
	U	4.71		Th	6.24	Ca	4.35
	K	0.61		U	2.04	Ti	0.0
	Ti	0.00	ppm	La	17.02	Fe	0.0
	Ca	2.91		Ce	33.43	U	75.79
	Fe	2.0		Pr	3.73		
ppm	Hf	3.06		Nd	11.41		
	Zr	64.01		Sm	0.79		
				Eu	0.19		
	Elements wt%	Betafites		Elements wt%	Uraninite	Elements wt%	Kasolite
	Al	1.3		Al	5.17	Al	2.55
	Si	4.11		Si	6.48	Si	8.96
	K	2.06		Ca	4.91	Pb	16.08
	Ca	0.0		Fe	1.37	U	72.41
	Ti	1.52		Pb	7.73		
	Fe	2.98		U	73.96		
	Ta	0.0					
	U	61.97					
	Nb	26.07					

The abundance distribution pattern of the major constituent of the studied granites shows a very limited variation with respect to alumina, as well as silica, and potassium. However, the rest of the major components display remarkable variation in abundance, especially for Fe_2O_3, MnO, CaO, Na_2O and P_2O_5 (Fig. 5). The above observations may suggest that alumina was the least mobile during Na-dominated metasomatic alteration processes, associated with a notable activity of the ferromanganese fluids.

The variation diagram of the trace elements (Fig. 6) suggests significant variation for most trace elements, especially uranium and the multivalent elements such as Cd, Mo, Pb, Cu, and Zn. The. high field strength elements display wide variation for their light isovalents, namely Nb and Zr, while the corresponding heavy isovalents (i.e., Ta and Hf) display a rather limited variation.

The major oxides of the studied granites are normalized to the average of Upper Continental Crust (Rudnick and Gao 2004), average Worldwide granites (Blatt and Tracy 1997) and the average of A-type granite from Brazil (Frederico et al. 2014). The normalization (Fig. 7) indicates that the studied granites have normal abundance with respect to SiO_2, Al_2O_3 and K_2O, but they are MnO-enriched and TiO_2-, MgO-, CaO- and Na_2O-depleted. It can be stated that the studied granites have highly fractionated major composition.

The comparison between the mean of the trace elements content of the studied granites and the (UCC) Upper Continental Crust (Rudnick and Gao 2004) suggest the following remarks:

1. The studied granites are distinctly anomalous in U, where the average U is more than 620-fold the UCC. The Th/U ratio decreases from 2.8, as a chondritic value, to 0.0023 for the studied granites. This proposes extreme fractionation towards an extensive secondary migration-in of U (Fig. 8).
2. There is marked enrichment (> tenfold) of the elements Cd, Mo, Pb, Bi, Nb and W (Fig. 8).
3. The high field strength elements (HFSE), such as Zr, Hf, Nb and Ta display peculiar distribution. The Zr and Hf are depleted in the studied granites relative to the UCC, whereas Nb and Ta are strongly enriched. The Zr/Hf ratio is about one, while it is supposed to be 35 for the chondritic value. This proposes that the zircon mineral in the studied granites is certainly Hf-rich and of secondary origin. Despite the clear enrichment of

Table 3 Complete chemical analyses of 30 fresh and metasomatized highly differentiated granites from El Maghrabi and EL Eredyia granitic plutons

Sample no	Mg (n = 7)	ER (n = 7)	ER3A	ER3B	ER3B	ER3D	DTT1	DTT2	DTT3	DTT4	DTT5	DTT6	DTT7	DTT8
Oxides %														
SiO_2	74.29	73.84	73.89	73.46	73.26	74.00	73.66	73.65	73.04	76.14	75.34	76.40	74.59	73.50
TiO_2	0.10	0.15	0.09	0.09	0.09	0.09	0.06	0.07	0.07	0.08	0.09	0.08	0.09	0.10
Al_2O_3	14.47	16.19	16.00	16.24	16.44	16.24	16.04	15.92	15.38	15.74	16.62	16.00	17.16	17.93
Fe_2O_3	0.75	0.99	2.32	2.36	2.38	2.34	1.36	1.41	1.39	0.93	0.90	0.94	0.77	0.79
MnO	0.05	0.03	0.05	0.04	0.04	0.04	1.68	1.79	1.79	0.01	0.01	0.01	0.17	0.18
MgO	0.15	0.09	0.07	0.05	0.07	0.05	0.07	0.07	0.07	0.05	0.05	0.05	0.07	0.07
CaO	0.48	0.46	0.17	0.17	0.17	0.17	0.07	0.69	0.70	0.04	0.04	0.04	0.08	0.08
Na_2O	5.06	2.26	0.08	0.09	0.08	0.08	0.08	0.07	0.07	0.08	0.08	0.09	0.22	0.22
K_2O	3.91	4.04	2.69	2.75	2.72	2.68	3.52	3.59	3.64	4.22	4.24	3.54	3.79	4.17
P_2O_5	0.04	0.03	0.04	0.37	0.37	0.03	0.02	0.02	0.02	0.01	0.01	0.01	0.01	0.02
SO3	< 0.1	< 0.1	0.23	0.23	0.23	0.25	< 0.1	< 0.1	< 0.1	0.13	< 0.1	0.15	< 0.1	< 0.1
LOI	0.69	1.92	4.62	4.39	4.38	4.27	3.45	2.72	3.84	2.68	2.62	2.82	3.04	2.94
Trace and Rare elements														
Li	11.70	9.65	13.50	12.90	14.40	14.90	21.90	20.20	21.00	15.00	16.90	15.30	14.50	15.00
Rb	73.85	157.50	120.90	123.60	123.80	120.30	133.80	129.80	133.10	152.00	157.20	126.20	148.90	156.00
Cs	1.10	1.65	2.00	2.00	2.10	2.00	1.10	1.00	1.10	1.00	1.00	0.90	1.30	1.30
Be	3.50	4.50	10.00	9.00	10.00	10.00	6.00	6.00	5.00	5.00	5.00	4.00	4.00	3.00
Sr	64.50	56.00	208.00	217.00	228.00	206.00	198.00	190.00	193.00	42.00	39.00	39.00	79.00	85.00
Ba	795.00	180.00	3702.00	3856.00	3768.00	3928.00	754.00	727.00	757.00	131.00	146.00	128.00	232.00	209.00
V	3.00	8.50	3.00	1.00	3.00	3.00	9.00	9.00	9.00	5.00	5.00	5.00	8.00	8.00
Ni	1.15	2.20	4.20	3.20	3.60	3.40	3.50	3.60	4.00	1.60	1.80	2.40	2.00	2.00
Cr	2.50	8.50	7.00	6.00	7.00	6.00	5.00	8.00	6.00	4.00	4.00	7.00	4.00	4.00
Co	0.50	1.30	2.40	2.40	2.20	2.30	8.70	8.50	8.70	0.80	1.00	0.90	3.00	3.60
Cu	5.50	5.65	32.10	28.60	32.00	29.70	8.30	8.30	8.20	6.10	9.30	8.20	4.70	5.00
Zn	77.30	52.85	504.90	533.60	516.90	523.40	203.10	203.90	210.80	72.50	89.50	73.80	103.60	101.70
As	2.20	3.80	34.10	35.80	37.90	34.50	4.00	3.60	2.70	2.90	2.60	2.70	2.60	3.50
Se	0.30	< 0.3	< 0.3	< 0.3	< 0.3	< 0.3	< 0.3	< 0.3	< 0.3	0.60	< 0.3	< 0.3	< 0.3	< 0.3
Mo	1.14	3.46	90.79	89.26	92.76	85.35	16.02	16.02	15.74	40.35	39.65	37.98	3.35	3.43
Cd	1.37	0.03	0.22	0.18	0.22	0.09	1.54	1.44	1.38	0.12	0.19	0.10	0.44	0.29
Sn	4.45	8.85	15.80	14.40	16.00	15.30	5.50	5.50	5.70	7.80	8.20	7.60	8.70	9.10
Sb	0.07	0.24	2.99	3.02	3.21	2.98	0.59	0.65	0.65	0.33	0.35	0.32	0.26	0.27
Pb	16.45	37.25	369.29	382.01	379.93	363.77	46.03	44.84	44.02	167.81	161.39	161.57	117.64	120.60
Bi	0.18	0.84	2.99	2.80	3.36	3.37	0.45	0.48	0.44	4.89	5.14	4.07	0.30	0.35
Ag ppb	<20	601.50	ND*	ND	ND	ND	466.00	513.00	462.00	1867.00	2022.00	1905.00	426.00	338.00

Table 3 continued

Sample no	Mg (n = 7)	ER (n = 7)	ER3A	ER3B	ER3B	ER3D	DTT1	DTT2	DTT3	DTT4	DTT5	DTT6	DTT7	DTT8
Sc	2.45	2.25	5.40	5.20	6.00	5.10	1.50	1.60	1.70	1.60	1.60	1.50	2.10	2.00
Y	16.30	39.80	60.00	58.20	66.60	55.70	84.60	90.70	93.20	21.90	21.90	22.40	28.20	27.80
La	8.05	11.50	8.90	9.10	9.30	8.90	6.50	6.50	6.70	6.80	6.10	6.50	8.00	16.00
Ce	20.47	27.11	27.16	26.79	28.07	26.61	11.65	11.71	12.32	12.75	11.59	12.88	15.30	23.88
Pr	2.55	3.45	3.20	2.90	3.00	3.00	2.10	2.10	2.20	2.10	2.20	2.20	2.40	2.90
Nd	9.75	15.15	13.20	14.20	13.60	12.90	11.20	10.50	10.60	9.60	9.70	9.30	9.80	11.20
Sm	2.80	4.35	3.90	3.70	4.10	3.80	4.70	4.40	4.20	2.50	2.40	2.50	2.60	2.40
Eu	0.60	0.45	0.50	0.30	0.40	0.20	0.50	0.50	0.50	0.30	0.30	0.30	0.30	0.30
Gd	2.45	4.15	4.50	4.30	4.70	4.90	6.30	6.80	6.60	2.60	2.90	2.80	3.50	2.50
Tb	0.40	0.80	0.90	1.00	0.90	0.80	1.30	1.50	1.50	0.40	0.40	0.40	0.50	0.50
Dy	2.95	6.10	7.20	7.80	7.20	6.50	10.90	11.80	10.70	2.70	3.30	3.40	4.40	3.60
Ho	0.55	1.10	1.70	1.70	1.80	1.70	2.80	2.60	2.70	0.60	0.70	0.80	0.90	0.80
Er	1.80	3.95	5.50	6.10	6.80	5.90	8.00	8.40	8.10	2.10	2.60	2.60	3.30	2.90
Tm	0.20	0.65	1.00	1.00	1.30	1.20	1.30	1.40	1.50	0.50	0.50	0.50	0.60	0.60
Yb	1.80	5.85	9.20	8.30	10.30	9.20	9.20	9.70	9.80	3.20	3.80	3.30	4.80	4.40
Lu	0.25	0.80	1.50	1.50	1.50	1.20	1.30	1.60	1.50	0.50	0.70	0.70	0.70	0.60
Ga	20.68	19.32	20.62	20.61	21.73	20.86	15.88	14.55	15.55	14.73	16.79	14.38	16.75	17.28
Tl	0.61	1.31	0.96	1.00	1.03	1.00	1.49	1.47	1.51	1.08	1.14	1.05	1.37	1.32
Zr	65.00	101.20	129.40	126.30	138.30	127.00	53.20	56.70	66.90	69.20	65.00	68.90	71.70	81.40
Hf	2.71	4.10	4.67	4.74	5.12	4.43	2.43	2.25	2.46	3.29	3.31	3.38	3.30	3.71
Nb	22.43	34.15	559.02	615.53	597.86	571.85	47.53	46.98	48.52	28.79	30.40	33.79	42.80	41.79
Ta	1.65	4.95	6.10	6.40	6.20	6.00	2.70	2.80	3.00	3.70	3.70	3.90	4.50	4.20
U	9.15	54.20	9020.00	9550.00	9320.00	9040.00	244.80	239.70	258.60	64.00	80.20	73.10	62.10	42.70
Th	5.55	18.60	16.30	15.50	16.10	16.20	9.40	9.30	9.30	13.30	15.10	14.40	14.00	15.50
W	0.95	1.00	137.40	143.30	143.90	137.00	4.60	4.60	4.70	0.80	1.10	0.80	1.70	1.20

Sample no	DTT9	DTT10	DTT11	DTT12	DTT13	DTT14	DTT15	DTT16	DTT17	DTT18	DTT19	DTT20	DTT21	DTT22	DETECTION
Oxides %															LIMIT (DL)
SiO_2	72.98	76.01	75.67	75.98	74.85	74.46	73.63	66.34	66.26	65.81	74.07	73.24	66.51	66.28	64.49
TiO_2	0.10	0.08	0.08	0.08	0.10	0.11	0.11	0.10	0.10	0.09	0.09	0.10	0.09	0.10	0.74
Al_2O_3	18.43	16.44	16.38	16.30	18.14	17.18	17.83	14.62	14.65	14.17	17.01	18.06	14.43	14.60	16.06
Fe_2O_3	0.73	0.76	0.84	0.84	0.84	0.81	0.79	2.64	2.75	2.72	0.80	0.86	2.67	2.75	6.22
MnO	0.20	0.05	0.06	0.05	0.07	0.08	0.09	7.95	7.84	8.54	0.08	0.09	7.91	8.01	0.14
MgO	0.07	0.07	0.07	0.07	0.03	0.03	0.03	0.13	0.13	0.13	0.03	0.03	0.13	0.13	1.30
CaO	0.08	0.07	0.07	0.07	0.04	0.04	0.04	0.24	0.24	0.24	0.04	0.04	0.24	0.24	4.92

Table 3 continued

Sample no	DTT9	DTT10	DTT11	DTT12	DTT13	DTT14	DTT15	DTT16	DTT17	DTT18	DTT19	DTT20	DTT21	DTT22	DETECTION
Na_2O	0.22	0.14	0.13	0.13	0.13	0.12	0.12	0.14	0.14	0.16	0.12	0.12	0.15	0.15	4.50
K_2O	4.14	3.39	3.42	3.42	2.78	4.16	4.29	2.77	2.93	2.76	4.70	4.39	2.91	2.84	0.70
P_2O_5	0.01	0.03	0.03	0.03	0.01	0.02	0.01	0.05	0.06	0.06	0.02	0.02	0.06	0.06	0.13
SO3	< 0.1	< 0.1	< 0.1	< 0.1	< 0.1	< 0.1	< 0.1	< 0.1	< 0.1	< 0.1	< 0.1	< 0.1	< 0.1	< 0.1	0.80
LOI	3.04	2.97	3.27	3.05	3.00	2.99	3.05	5.00	4.91	5.32	3.03	3.06	4.90	4.85	100.00
Trace and Rare elements															
Li	13.90	13.40	13.00	13.80	8.50	9.50	9.30	11.10	11.50	11.30	8.30	9.70	11.20	11.60	0.10
Rb	157.90	139.40	133.60	142.70	122.70	162.80	167.20	119.40	125.90	122.90	176.80	167.90	124.70	125.90	0.10
Cs	1.20	1.10	1.00	1.10	1.60	1.50	1.50	1.70	1.80	1.80	1.50	1.50	1.80	1.80	0.10
Be	3.00	4.00	4.00	4.00	4.00	4.00	3.00	19.00	16.00	17.00	3.00	4.00	17.00	20.00	1.00
Sr	74.00	58.00	55.00	64.00	64.00	66.00	61.00	1372.00	1521.00	1536.00	64.00	66.00	1473.00	1596.00	1.00
Ba	176.00	134.00	134.00	157.00	160.00	153.00	139.00	3146.00	3403.00	3590.00	144.00	154.00	3508.00	3696.00	1.00
V	8.00	7.00	7.00	6.00	4.00	5.00	4.00	21.00	24.00	23.00	5.00	5.00	24.00	23.00	1.00
Ni	1.90	3.10	3.40	3.40	1.70	1.50	2.40	11.80	11.40	12.00	1.60	3.00	12.20	11.80	0.10
Cr	4.00	4.00	4.00	4.00	4.00	4.00	3.00	7.00	8.00	8.00	3.00	5.00	7.00	9.00	1.00
Co	3.10	3.20	3.50	3.70	1.60	1.50	2.20	46.30	48.80	48.70	1.40	2.20	48.00	50.00	0.20
Cu	5.00	4.40	4.50	5.30	2.30	2.10	9.80	59.00	60.00	61.50	1.80	11.50	63.00	62.70	0.10
Zn	101.70	111.90	112.70	107.60	87.20	82.90	106.00	1125.90	1158.10	1174.60	83.50	109.20	1135.70	1184.60	0.20
As	3.20	9.50	9.70	10.40	2.00	2.10	2.30	11.80	11.10	12.40	2.80	2.70	11.10	10.50	0.20
Se	< 0.3	0.50	< 0.3	0.30	< 0.3	< 0.3	< 0.3	2.00	1.00	1.50	< 0.3	< 0.3	1.50	1.20	0.30
Mo	2.90	2.68	2.98	3.13	2.23	2.02	1.91	90.81	93.04	99.16	2.02	2.02	96.31	98.86	0.05
Cd	0.28	0.15	0.27	0.20	0.13	0.13	0.25	11.26	11.98	12.23	0.12	0.24	11.76	13.14	0.02
Sn	9.50	9.10	8.40	9.40	8.40	8.50	8.00	6.80	7.10	7.60	9.30	8.70	6.40	7.10	0.10
Sb	0.23	0.49	0.49	0.45	0.18	0.20	0.20	2.64	2.71	2.84	0.21	0.19	2.70	2.90	0.02
Pb	102.11	83.68	89.24	91.30	44.85	42.18	39.38	664.91	673.83	690.61	41.85	41.84	662.34	746.04	0.02
Bi	0.29	0.46	0.41	0.41	0.35	0.33	0.31	3.85	4.35	5.19	0.39	0.34	4.25	5.48	0.04
Ag ppb	407.00	ND	ND	ND	368.00	342.00	360.00	ND	ND	ND	357.00	295.00	ND	ND	20.00
Sc	2.00	2.20	2.30	2.80	1.90	1.90	2.00	5.70	5.30	5.30	1.90	1.80	5.10	5.20	0.10
Y	29.40	141.70	138.00	159.00	24.50	24.70	22.70	466.60	462.20	471.40	25.40	24.00	518.40	471.20	0.10
La	7.90	7.50	7.20	8.10	8.90	10.70	9.10	18.80	20.30	22.40	9.30	9.00	19.80	20.30	0.10
Ce	14.79	18.03	19.68	20.88	21.62	25.24	19.84	49.10	51.59	56.56	22.61	21.23	50.96	53.71	0.02
Pr	2.60	2.80	2.60	2.90	2.50	2.80	2.40	13.20	13.70	14.90	2.50	2.50	14.10	14.50	0.10
Nd	9.30	12.80	12.50	14.50	11.10	11.70	9.00	74.50	74.20	83.50	10.60	9.70	77.10	76.60	0.10
Sm	2.90	7.80	7.60	8.20	2.40	2.70	2.10	32.00	34.10	35.90	2.40	2.40	34.70	36.40	0.10

Table 3 continued

Sample no	DTT9	DTT10	DTT11	DTT12	DTT13	DTT14	DTT15	DTT16	DTT17	DTT18	DTT19	DTT20	DTT21	DTT22	DETECTION
Eu	0.30	1.00	1.10	1.00	0.30	0.20	0.20	4.10	3.90	4.40	0.20	0.20	3.80	3.90	0.10
Gd	2.90	12.60	11.60	11.90	2.70	2.70	2.40	40.00	44.50	43.60	3.00	2.10	42.20	44.80	0.10
Tb	0.50	2.50	2.40	2.60	0.50	0.40	0.40	8.70	9.10	9.20	0.40	0.40	9.20	9.20	0.10
Dy	4.20	19.30	18.00	21.20	3.80	2.90	3.50	61.70	66.90	71.00	3.90	3.30	67.40	67.20	0.10
Ho	1.00	4.30	4.10	4.70	0.70	0.80	0.90	13.80	14.30	14.80	0.70	0.80	14.40	15.80	0.10
Er	3.20	15.70	14.30	16.60	2.90	2.30	2.60	46.10	45.30	48.00	2.60	2.80	48.10	47.50	0.10
Tm	0.50	2.50	2.20	2.50	0.40	0.40	0.40	7.00	7.10	7.50	0.50	0.40	7.70	7.30	0.10
Yb	4.40	19.00	16.40	18.70	3.00	3.50	3.00	50.50	49.60	51.20	3.80	3.60	52.20	48.10	0.10
Lu	0.60	2.60	2.40	2.80	0.60	0.50	0.50	6.60	7.10	6.90	0.50	0.60	7.40	7.70	0.10
Ga	16.39	16.58	17.28	17.58	18.76	17.69	18.06	21.41	20.94	22.75	18.42	18.02	21.65	23.21	0.02
Tl	1.18	1.11	1.02	1.02	1.34	1.30	1.25	4.74	4.77	4.94	1.29	1.23	4.97	5.15	0.05
Zr	63.20	112.50	114.20	113.70	60.10	66.20	57.50	293.70	303.80	334.00	65.40	60.00	321.70	328.30	0.20
Hf	3.15	3.14	3.22	3.42	3.08	3.01	2.97	3.89	3.48	3.94	3.20	2.97	3.66	3.63	0.02
Nb	37.90	181.02	179.51	206.95	32.04	30.47	34.03	877.58	1078.14	1056.43	30.95	33.61	1088.44	1168.36	0.04
Ta	4.50	3.80	3.30	4.00	4.00	3.90	4.00	2.10	2.70	2.60	3.80	4.40	2.50	2.50	0.10
U	41.10	324.00	355.00	383.00	25.00	18.50	15.50	2255.30	2103.50	2179.00	19.30	15.20	2082.80	2180.10	0.10
Th	14.70	13.20	13.20	14.20	16.10	17.30	15.10	20.10	20.20	21.00	15.50	14.70	20.90	21.10	0.10
W	1.20	5.10	5.20	6.30	1.20	0.90	1.00	29.40	29.20	30.10	1.00	1.10	30.40	31.70	0.10

All trace and rare elements in (ppm), except for Ag (ppb); n.m—not measured; ND—under detection limit; sample no Mg11–Mg18 (El Maghrbia fresh granite); sample no ER14-ER25 (El Eredyia fresh granite); sample no ER3A: ER3C and DTT1: DTT22 (El Eredyia altered granite); all samples are surface samples except all DTT samples are Sub surface samples

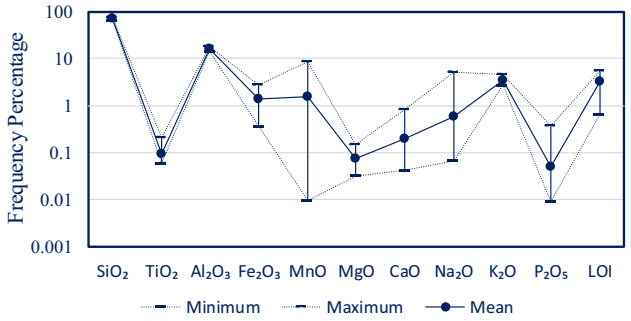

Fig. 5 Variation diagram of major components of the studied "fresh" and altered granites

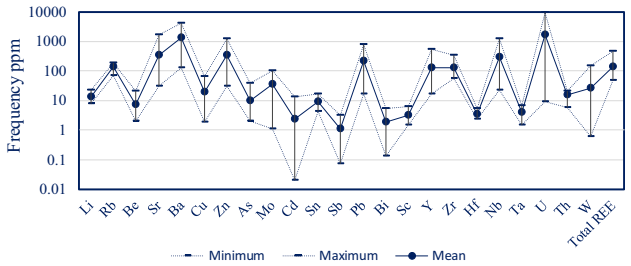

Fig. 6 Variation diagram of trace elements of the studied "fresh" and altered granites

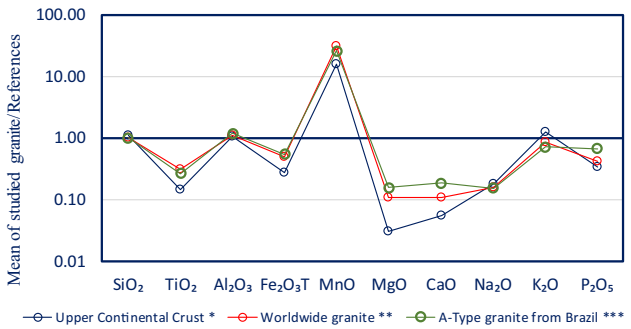

Fig. 7 Mean major oxides of the studied granites normalized to Upper Continental Crust, worldwide granites and A-type granite from Brazil

both Nb and Ta, they display clear fractionation as isovalents. The Nb/Ta ratio measures 5.8 instead of 17.6 for chondritic value (Weyer et al. 2002).

4. The total REE budget is almost similar to that of the UCC, whereas the content of Y is about sixfold enriched. This possibly reflects relative enhancement of the HREE during the alteration processes (Fig. 8).
5. Limited depletion has been recorded for a few elements including Li, Cu and Sc, in addition to Zr and Hf.

6 Discussions

6.1 Alterations and mineralizations

The mineralizations are structurally controlled by shear zones in the southern part of El Eredyia granites. More than one generation of quartz veins are occur, but the mineralizations are associated with the jasperoid and smoky veins, which occupy faults at the centre of the shear zones. The shear zones are characterized by specific alteration zoning around the mineralizations. The alterations include mainly silicification, kaolinization, and slightly altered granite passes gradually to fresh granite. Also, other alterations are developed on the main faults or just around them, including ferrugination, less abundant limonitization, black manganese and iron oxide stainings, and some argillic materi-als. They are most probably of hydrothermal nature. The mineralizations show a preferable developement at the marginal zones of the pink granite mass. The uranium minerals occur in three modes of occurrence; as stains on the hanging wall of the jasperoid veins, as disseminations in microfractures branching from the main fault, and between the intersecting of faults. Intense oxidation and leaching processes affected the primary uranium minerals which have caused either the complete oxidation of the primary mineral into the secondary minerals or complete leaching of uranium minerals.

6.2 Geochemical correlations

The correlations among more than 50 variables in 30 "fresh" and altered granite samples suggest important geochemical inferences. The alteration of granites steered abnormal accumulation of some rare metals particularly uranium. The content of uranium is up to about 1% in four samples. Uranium correlates with $Fe_2O_3^T$, suggesting a possible association between uranium and ferrugination. Uranium correlates also with some redox-sensitive elements such as Mo, As, Sn and Sb (Fig. 9).

The behavior of the high field strength elements (HFSE) is very peculiar, where the two light isovalents (i.e., Zr and Nb) display strong dependence, whereas the two heavy isovalents (i.e., Hf and Ta) are not correlated (Fig. 10). The Zr/Hf and Nb/Ta ratios seem to be non-charge and radius controlled where their correlations confirm availability of both Hf-depleted and Hf-enriched zircon. Likewise, the plot of Nb and Ta endorses the availability of both Ta-poor and Ta-enriched columbite.

Contrarily, the two isovalents Y and Ho do not show differentiation, where their ratio measures about 32, which is close to the chondritic value (28). Moreover, Y correlates strongly with the total REE budget (Fig. 11). Eventually,

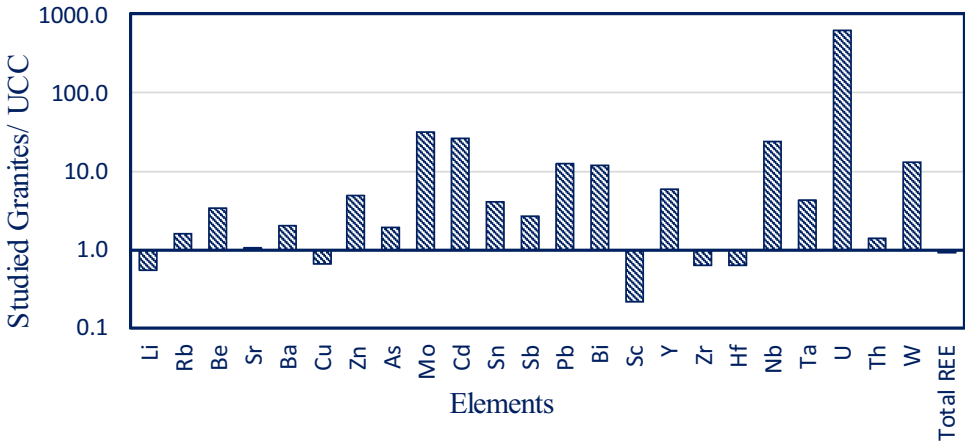

Fig. 8 Average trace elements content of the studied granites normalized to the Upper Continental Crust (UCC) as quoted by Rudnick and Gao (2004)

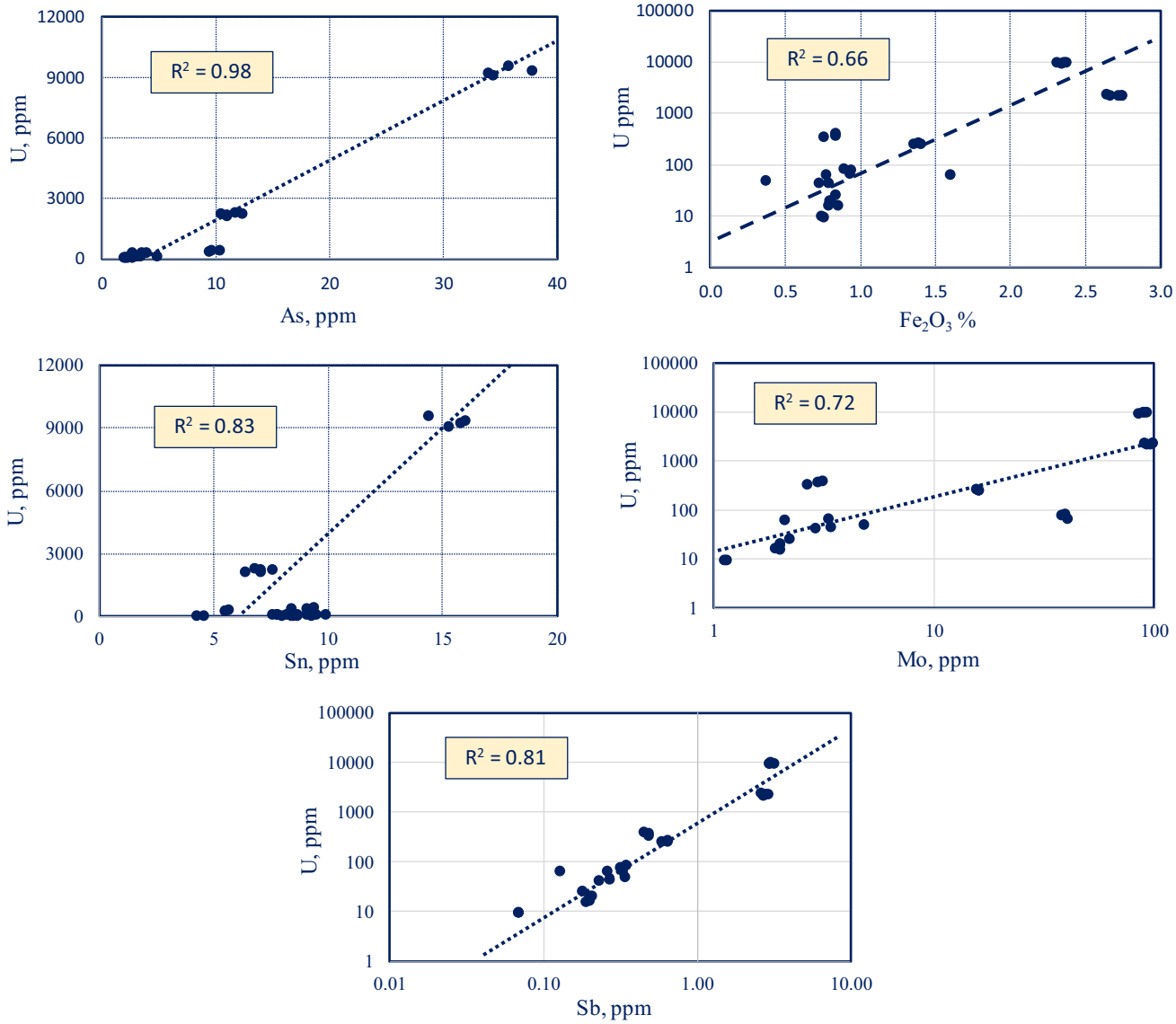

Fig. 9 Correlations between U and redox-sensitive elements including Fe, As, Sn, Sb and As

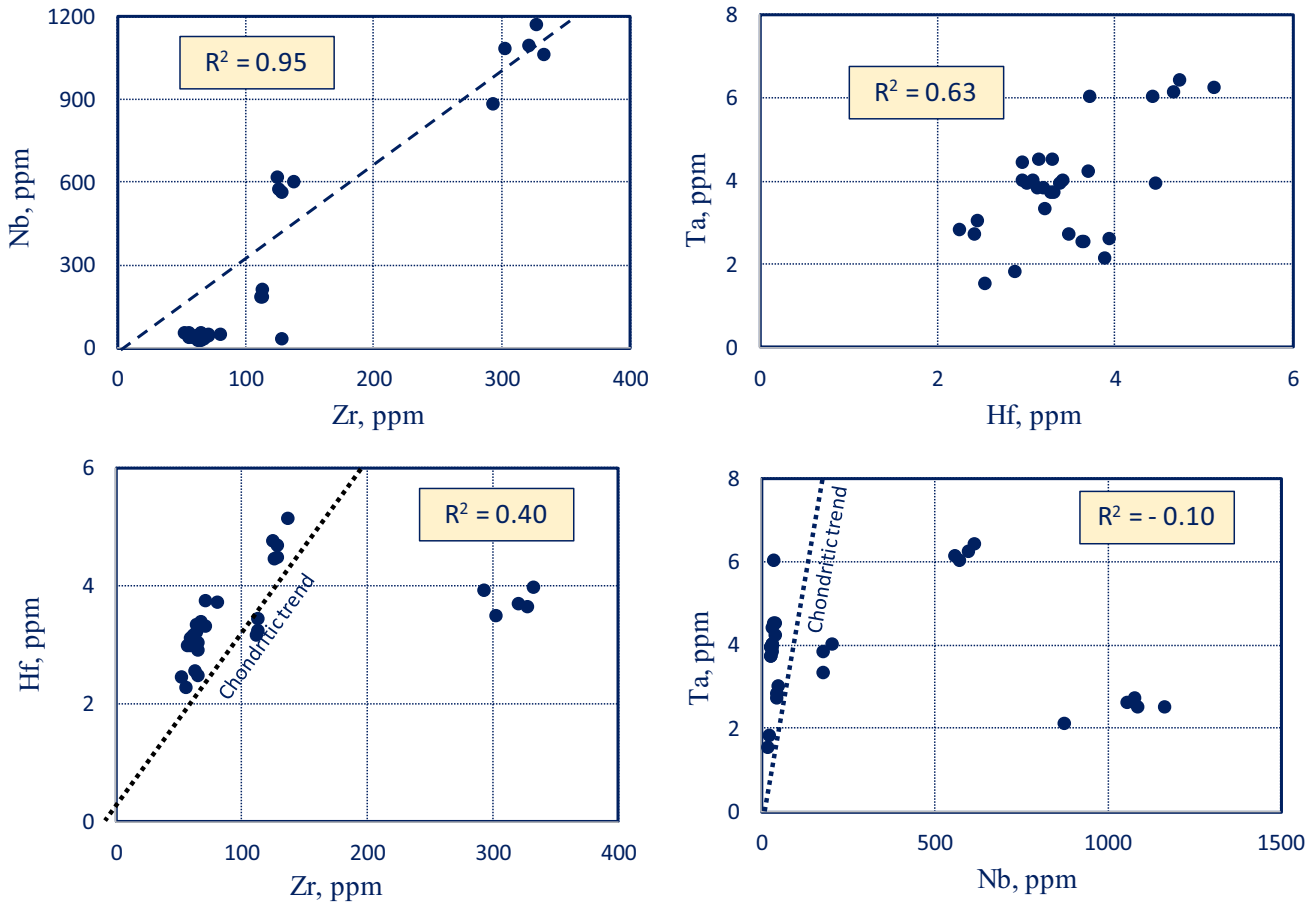

Fig. 10 Correlations among the main high field strength elements in the studied "fresh" and altered granites

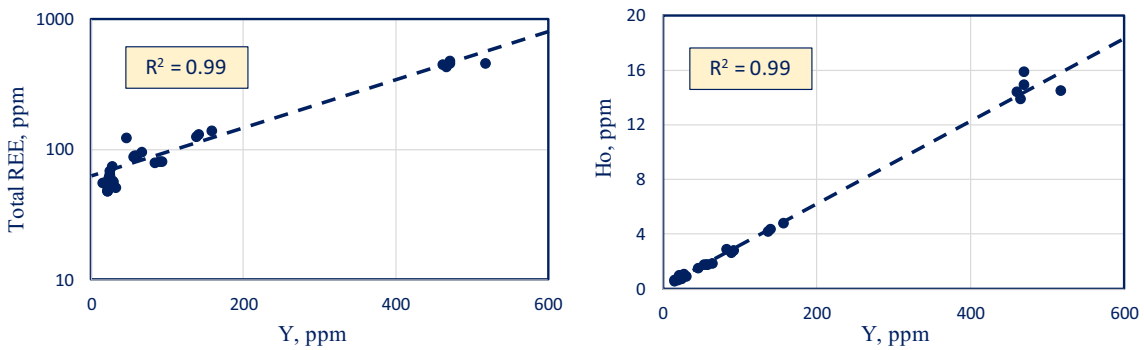

Fig. 11 Strong correlations between Y and both total REE and Ho, as a heavier isovalent

ferruginous material seems to be an influential accumulator of heavy metals and uranium. Fe_2O_3 displays good correlations with Zn, Mo, Pb, Cu (Fig. 12), among others. The petrographic examination of the studied granite suggests that the ferruginous material is a secondary product of either pseudomorphic oxidation of pyrite precursor or exsolution of Fe_2O_3 during muscovitization. The heavy metals, and uranium, keep an intimate coherence to the ferruginous material possibly through sorption or scavenging mechanisms.

7 Conclusions and recommendation

Field investigation revealed that the exposed rocks in the studied area are chronologically arranged from the oldest by metavolcanics, granodiorites, younger gabbros,

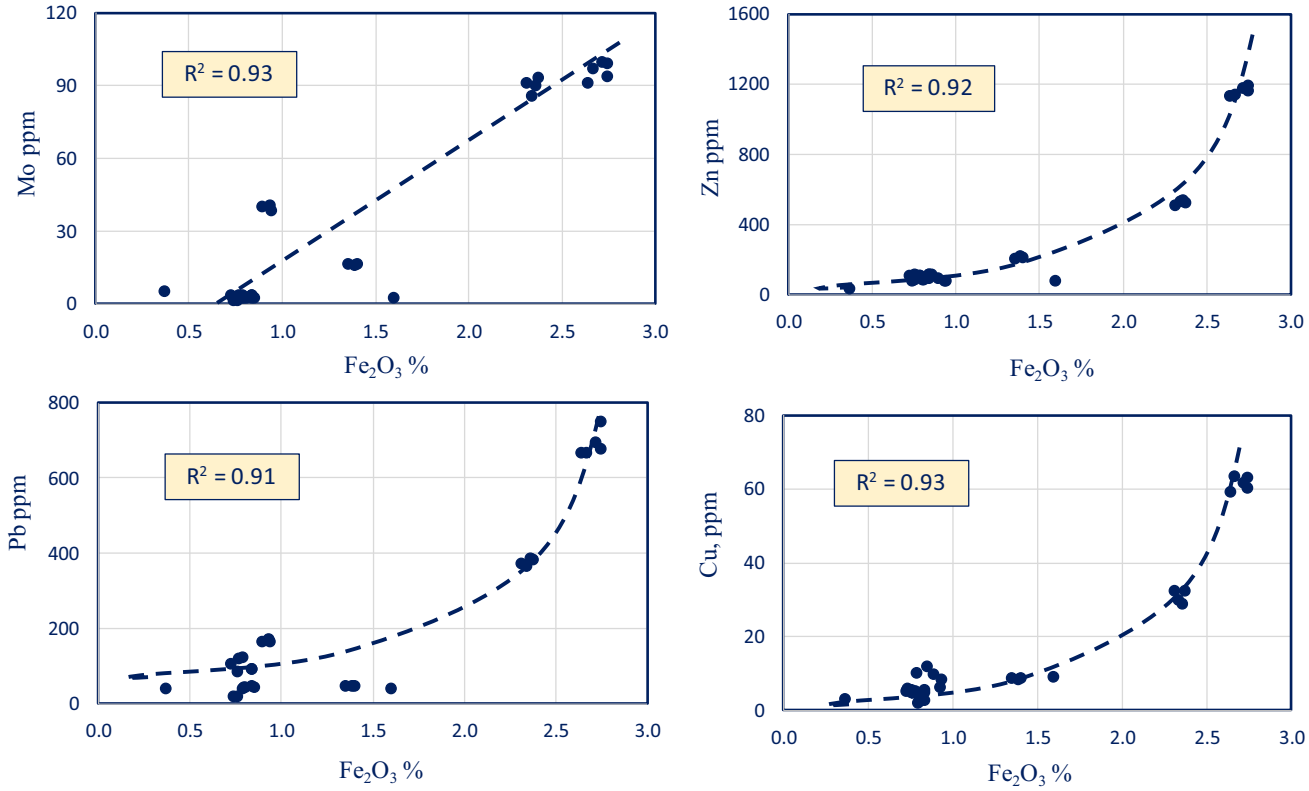

Fig. 12 Strong correlations between Fe_2O_3 and some heavy metals

monzogranites and dikes. The studied area is one of the most promising localities at Nuclear Materials Authority owing to the presence of uranium occurrences.

Petrographical and mineralogical examination illustrate that alteration process occurred in three phases. First phase comprise silicification, kaolinitization, sassuritization and ferrugination are the most common alteration features along major and minor fractures, the second phase of alteration is indicated by rejuvenation of these fractures as indicated by normal faults and by brecciation of the early silica veins as well as the intrusive contacts of this granite andalteration of pitchblende and iron oxides indicates a third alteration event and redistribution process which leached uranium from some of the altered zones, especially the friable unsilicified ones, while the original mineralization is preserved in silicified zones. Most of the high uranium concentrations are associated with the second alteration phase in the cementing red silica of the brecciated contacts, and with the third phase in the alteration zones at the jasperoid veins intersections with the secondary fractures. G. El-Erediya monzogranites have higher contents of their radioactivity than in El Maghrbia monzogranites due to the presence of radioactive minerals as uranothorite Uranophane, Uraninite, Betafite and Kasolite.

Geochemically, there is marked enrichment (> tenfold) of the elements Cd, Mo, Pb, Bi, Nb and W and the high field strength elements (HFSE), such as Zr, Hf, Nb and Ta display peculiar distribution. The Zr and Hf are depleted in the studied granites relative to the UCC, whereas Nb and Ta are strongly enriched. The behavior of the high field strength elements (HFSE) is very peculiar, where the tow light isovalents (i.e., Zr and Nb) display strong dependence, whereas the two heavy isovalents (i.e., Hf and Ta) are not correlated.

Consequently, we recommended to evaluate the investigated mineralized monzograintes by selective some technological samples in order estimate the preserve of radioactive minerals as well as precious economic rate-metal mineralization.

References

Abdallah SM (2004) Geological and mineralogical studies on some surface and subsurface sections from El-Missikat and El-Erediya uranium occurrences, Central Eastern Desert, Egypt. Ph.D. Thesis, Ain Shams Univ., p 219

Abd El-Naby HH (2007) Genesis of secondary uranium minerals associated with jasperoid veins, El Erediya area, Eastern Desert, Egypt. Miner Deposita 43:933–944

Abdel Meguid AA (1986) Geologic and radiometric studies of uraniferous granites in Um Ara-Um Shilman area south Eastern

Desert, Egypt. Unpub. Ph.D. Thesis, Univ. f Suez Canal, Egypt, p 233

Abu Dief A (1992) The relation between the uranium mineralization and tectonics in some Pan-African granites, west of Safaga, Eastern Desert, Egypt. Ph.D. Thesis. Assiut Univ., Egypt, p 218

Ali BH (2015) SHRIMP U-Pb zircon geochronology: evidence for emplacement time of some granitoids north Eastern Desert, Egypt. Arab J Geosci 8:5465–5474

Ali BH, Wilde SA, Gabr MMA (2009a) Granitoid evolution in Sinai, Egypt, based on precise SHRIMP U-Pb zircon geochronology. Gondwana Res 15:38–48

Ali KA, Stern RJ, Manton WI, Kimura JI, Khamees HA (2009b) Geochemistry, Nd isotopes and U-Pb SHRIMP zircon dating of Neoproterozoic volcanic rocks from the Central Eastern Desert of Egypt: New insights into the ~ 750 Ma crust-forming event. Precambr Res 171(1–4):1–22

Ali KA, Moghazi AKM, Maurice AE, Omar SA, Wang Q, Wilde SA, Moussa EM, Manton WI, Stern RJ (2012) Composition, age, and origin of the ~ 620 Ma Humr Akarim and Humrat Mukbid A-type granites: no evidence for pre-Neoproterozoic basement in the Eastern Desert, Egypt. Int J Earth Sci 101(7):1705–1722

Andresen A, Abu El Enen MM, Stern RJ, Wilde SA, Ali KA (2014) Wadi Zaghra metasediments of Sinai, Egypt: new constraints on the late Cryogenian-Ediacaran tectonic evolution of the northernmost Arabian-Nubian Shield. Int Geol Rev 56:1020–1038

Bakhit FS (1978) Geology and radioactive mineralization of G. El Missikat area, Eastern Desert: Ph. D. Thesis, Ein Shams Univ., Cairo, 289 p 7

Be'eri-Shlevin Y, Katzir Y, Whitehouse MJ (2009) Post-collisional tectono-magmatic evolution in the northern Arabian Nubian Shield (ANS): time constraints from ionprobe U-Pb dating of zircon. J Geol Soc Lond 166:1–15

Blatt H, Tracy RJ (1997) Petrology, 2nd edn. Freeman, New York, p 66

Cuney M, Le fort P, Wang ZX (1984) Uranium and Thorium Geochemistry and Mineralogy in the Manasluleucogranite (Nepal, Himalaya). Geology of Granites and Their Metallogenetic Relations (Proceedings of a Symposium), Nanjing, 1982, University Sceinces Editions, pp 853–873

Dardier AM (2004) Morphology, chemistry and U-contents of biotite flakes of the older granitoids and younger granites, Gabal El-Maghrabiya area, Eastern Desert, Egypt. Delta J Sci 28:1–18

Dardier AM, Hammad HM, Moharem AF (2001) Genesis of uranium in the younger granites of Gabal El-Maghrabiya area, central Eastern Desert, Egypt. J Min Soc Egypt 13:83–100

El Kassas IA (1974) Radioactivity and geology of Wadi Atalla area. Eastern Desert of Egypt, Arab Republic of Egypt. Ph. D. Thesis, Faculty of Science, Ein Shams University, Cairo, Egypt

El-Bialy MZ, Eliwa HA, Mahdy NM, Murata M, El-Gameel KH, Sehsah H, Omar M, Kato Y, Fujinaga K, Andresen A, Thomsenh TB (2020) U-Pb zircon geochronology and geochemical constraints on the Ediacaran continental arc and post-collision Granites of Wadi Hawashiya, North Eastern Desert, Egypt: insights into the ~ 600 Ma crust-forming Event in the northernmost part of Arabian-Nubian Shield. Precambr Res 345:105777

Eliwa HA, Breitkreuz C, Murata M, Khalaf IM, Buhler B, Itaya T, Takahashi T, Hirahara Y, Miyazaki T, Kimura JI, Shibata T, Koshi Y, Kato Y, Ozawa H, Daas MA, El Gameel Kh (2014) SIMS zircon U-Pb and mica K-Ar geochronology, and Sr-Nd isotope geochemistry of Neoproterozoic granitoids and their bearing on the evolution of the north Eastern Desert, Egypt. Gondwana Res 25:1570–1598

Eyal M, Litvinovsky B, Jahn BM, Zanvilevich A, Katzir Y (2010) Origin and evolution of post-collisional magmatism: coeval Neoproterozoic calc-alkaline and alkaline suites of the Sinai Peninsula. Chem Geol 269(3–4):153–179

Farahat ES, Zaki R, Hauzenberger C, Sami M (2011) Neoproterozoic calc-alkaline peraluminous granitoids of the Deleihimmi pluton, Central Eastern Desert, Egypt implications for transition from late- to post-collisional tectonomagmatic evolution in the northern Arabian-Nubian Shield. Geol J 46(6):544–560

Friedrich MH, Cuney M, Cregu G (1989) Uranium enrichment processes in Peraluminous Magmatism. International Atomic Energy Agency (IAEA)-TC-571/2.11-35

Jiashu R, Zehong H (1982) Forms of uranium occurrence and its distribution in uraniferous granites. In: Geology of granites and their metallogenetic relations. Sciences Press, Beijing, pp 621–635

Mahdy NM, El Kaliobi BA, Wohlgemuth Ueberwasser CC, Shalaby MH, El Afandy AH (2015) Petrogenesis of U- and Mo-bearing A2-type granite of the Gattar batholiths in the Arabian Nubian Shield, Northeastern Desert, Egypt: evidence for the favorability of host rocks for the origin of associated ore deposits. Ore Geol Rev 71:57–81

Maurice YT (1982) uraniferous granite and associated mineralization in the Fury and Hecla Strait area, Baffin Island, N.W.T. In: "uranium in granite" paper 81–23. Proceedings of a workshop held in Ottawa, Ontario, 25–26 November. 1980, pp 101–115

Moussa EM, Stern RJ, Manton WI, Ali KA (2008) SHRIMP zircon dating and Sm Nd isotopic investigations of Neoproterozoic granitoids, Eastern Desert, Egypt. Precambr Res 160(3–4):341–356

Poty B, Cuney M, Friedrich M (1986) Uranium deposits spatially related to granites in the French Part of the Hercynian Orogeny, Vein Type Uranium Deposits. IAEA-TECDOC-361, IAEA, Vienna, pp 215–246

Raslan MF (2009) Mineralogical and minerallurgical characteristics of samarsakite-y, columbite and zircon from stream sediments of the ras baroud area, Central Eastern Desert. The Scientific papers of the Institute of mining of the Wroclaw University of technology, Wroclaw, Poland, No. 128. Mining and GeologyXII, pp 179–195

Rudnick RL, Gao S (2004) The composition of continental crust. In: Rudnick RL (ed) Treatise on geochemistry, vol. 3, the crust. Elsevier, Amsterdam, pp 1–64

Salman AB, El Aassy IE, Shalaby MH (1990) New occurrence of uranium mineralization in GabalGattar, northern Eastern Desert, Egypt. Ann Geol Surv Egypt 16:31–34

Stern RJ, Hedge CE (1985) Geochronologic and isotopic constraints on Late Precambrian crystal evolution in the Eastern Desert of Egypt. Am J Sci 285:97–127

Streckeisen A (1976) To each plutonic rock its proper name. Earth Sci Rev 12:1–33

Weyer S, Münker C, Rehkämper M, Mezger K (2002) Determination of ultra-low Nb, Ta, Zr and Hf concentrations and the chondritic Zr/Hf and Nb/Ta ratios by isotope dilution analyses with multiple collector ICP-MS. Chem Geol 187:295–313